Power and Data Transmission for Wireless Electroceutical System

Joonyoung Lim and Yoon-Kyu Song[a]
Graduate School of Convergence Science and Technology, Seoul National University
Research Institute for Convergence Science
E-mail: limjoony@snu.ac.kr, songyk@snu.ac.kr

***Abstract* – This paper reviews the design concepts and constraints of current wireless power and data transmission technologies (e.g., inductive coupling, optical transmission, and ultrasonic-based techniques), and concentrates on the design and implementation of the proposed inductive coupling method for electroceutical applications. Especially considering miniaturisation and biocompatibility, our approach has the potential to become a competitive therapeutic alternative in many clinical settings in the future, since it guarantees more stable data communication and higher power transfer efficiency than current techniques. The chip is fabricated using the TSMC 180 nm CMOS process, and the size is 1 mm x 1 mm.**

***Keywords* – Wireless power and data transmission, electroceuticals, distributed systems.**

I. INTRODUCTION

Electroceuticals have recently emerged as a promising alternative to traditional drug therapy. While conventional drugs are delivered systemically, electroceuticals use targeted electrical impulses to stimulate or modify specific nerve bundles or tissue regions. This method seeks to deliver more targeted therapies that can minimize adverse effects and enhance therapeutic efficacy for many conditions, including neurological, metabolic, and inflammatory disorders [1].

One of the key challenges in developing effective electroceutical devices is ensuring a reliable power supply and communication without relying on bulky or disposable batteries. Batteries can constrain the dimensions and adaptability of implants, and they may be expensive, hazardous, or painful for patients due to the necessity of regular replacement. To address this, researchers are exploring wireless power transfer technologies that can provide the necessary energy while minimizing invasive procedures and reducing device size [2], [3], [4].

Fig. 1 presents the latest approaches to wireless electroceutical devices. Wireless power and data transmission technologies include inductive coupling, optical transmission, and ultrasound-based methods, each offers unique advantages in power efficiency, tissue penetration, and alignment tolerance but also has its own limitations. Optical technologies can provide exceptionally high data rates; nevertheless, they are constrained by restricted tissue penetration and associated heat accumulation concerns. Ultrasound-based devices may penetrate deeply into the body; yet, they may encounter signal attenuation and alignment challenges due to the intricate nature of tissue layers.

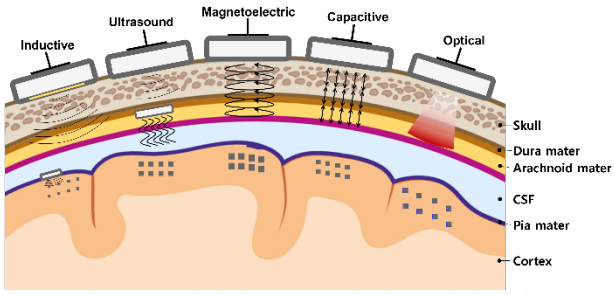

Fig. 1. Various types of wireless communication methods of electroceutical devices

However, inductive coupling is gaining popularity in implantable devices due to its excellent short-range energy transfer efficiency and reliable data communication. Advances in microfabrication techniques and high-frequency antenna design have enabled the integration of power management circuitry, stimulation drivers, and sensor interfaces into a single compact device. These distributed electroceutical networks can precisely stimulate specific nerves, such as the vagus nerve, with minimal invasiveness. Current research focuses on improving long-term biocompatibility, optimizing closed-loop feedback control, and developing personalized stimulation protocols, which have the potential to transform the treatment of a variety of diseases.

In this work, we systematically review the design concepts and constraints of current wireless power and data transmission technologies (e.g., inductive coupling, optical transmission, and ultrasonic-based techniques), and concentrate on the design and implementation of the proposed inductive coupling method for electroceutical applications. In particular, our approach, which considers miniaturization and biocompatibility, has the potential to develop into a competitive therapeutic option in various clinical environments in the future, as it enables higher power transfer efficiency and more stable data communication than existing methods.

a. Corresponding author: songyk@snu.ac.kr

Manuscript Received Apr. 8, 2025, Revised May 19, 2025, Accepted Jun. 10, 2025

II. EXPERIMENTS

A. Inductive Coupling

Inductive coupling provides high power transmission efficiency and stable data communication in short distances, and has the advantage of minimizing the spatial constraints of implantable devices through ultra-small antenna design. It is appropriate for the design of small implantable electroceutical devices, especially since it can transmit energy while minimizing interference with human tissue by using magnetic flux coupling. The newly proposed coil compensation technique can further increase transmission efficiency, and it also has the advantage of being able to control the balance between heat suppression and securing data bandwidth depending on frequency selection. Conversely, efficiency can drop quickly in limited transmission distances and large coil alignment deviation, thus, in real-world clinical settings the physical location of the transmitting and receiving coils must be exactly controlled [5], [6], [7].

B. Ultrasound Coupling

The ultrasound method has the advantage of relatively high tissue penetration, allowing power transmission even when the implantable device is placed deep in the body. Furthermore, although the driving frequency can be changed to fit different tissue environments, signal attenuation and reflection resulting from passing through different heterogeneous tissues may lower the efficiency. In particular, as the transducer becomes smaller, the transmission performance deteriorates rapidly even if the transmission and reception alignment is slightly misaligned, so resonance structure optimization and array design are essential for stable ultrasound transmission [8].

C. Magnetoelectric Coupling

The magnetoelectric technique can expect high energy conversion efficiency through the combination of electromagnetic fields and piezoelectric phenomena. Particularly when resonance takes place at a particular frequency, the device volume can be lowered while obtaining rather high power; however, there are drawbacks in that the multilayer structure must be precisely manufactured in an ultra-small unit and the formation and control of the external magnetic field is challenging. In addition, since temperature changes or micro-vibrations inside the human body can affect the magnetostriction coefficient, encapsulation technology to maintain it stably for a long period of time is also pointed out as an important task [9], [10].

D. Capacitive Coupling

Capacitive transmission has a simple structure and can be efficient under certain conditions, but the electrolyte environment inside the human body can cause significant interference in the transmission path between electrodes. Miniaturizing the transmission plate (electrode) improves the convenience of implantation, but circuit loss and distortion increase due to body fluids, making it difficult to maintain transmission efficiency. In addition, even if interference is mitigated through protective coating or electrode surface treatment, there is a risk of heat generation or tissue damage when operating at high voltages. For this reason, there are significant limitations on electrode placement and frequency control for stable power and data transmission [11].

E. Optical Coupling

Optical methods may have advantages over other techniques in terms of high-speed data transmission and wide bandwidth, but the large scattering and absorption of human tissue significantly limit the penetration distance. In addition, when using laser or LED-based light sources, beam alignment is very important to reduce optical loss, and poor heat dissipation design can cause thermal damage to adjacent tissues. When mounting ultra-small sensors and photodetectors, an amplifier circuit is required to increase the light detection efficiency, which also increases the overall volume [12].

In conclusion, the wireless power and data transmission technologies presented above each have their own advantages and limitations. However, in this study, the inductive coupling method was adopted by comprehensively considering the advantages of high-power transmission efficiency in short distances, stable communication, and easy optimization when implementing small implantable devices.

F. System Design

ANSYS HFSS was used to design and simulate the antenna coil structure; the model chosen was meant to maximise the Q factor. The antenna efficiency, resonant frequency matching, and matching circuits were further validated using the Cadence Design Simulator, with simulation data extracted from HFSS. The simulation model, shown in Fig. 2 (a), is a designed antenna 1 mm × 1 mm, which incorporates the dielectric properties of substrate silicon, an oxide layer, a polysilicon layer, and metal layers. With the relay coil positioned in the CSF layer, a multi-layer tissue model was built for the in-vivo dielectric conditions: 1 mm of skin, 0.14 mm of fat, 7 mm of skull, 0.5 mm of dura, 0.2 mm of cerebrospinal fluid (CSF), and 81 mm of grey matter. Figure 2 (a) shows modeling of the coil antenna using metal layers in HFSS and tissue layers beneath.

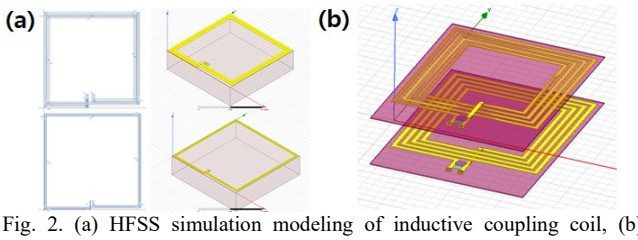

Fig. 2. (a) HFSS simulation modeling of inductive coupling coil, (b) simulation setup for coil-to-coil wireless transmission

Fig. 2 (a) shows modeling of the coil antenna using metal layers in HFSS, and applied over the tissue layers for

simulation. The on-chip coil size was optimized to maximize coil efficiency while making full use of the available area within the 1 mm × 1 mm chip boundary. Fig. 2 (b) shows the antenna matching simulation model, and to assess matching efficiency, simulations were conducted with the antennas positioned facing each other. To fit within the CMOS fabrication area, a 2-turn coil construction was selected. The width and spacing of the metal were varied to maximize coil efficiency at the 915 MHz transmission frequency. The frequency 915 MHz was chosen to reduce tissue absorption and guarantee enough power supply to the small-sized coils. The on-chip coil was fabricated using Metal 6 in the TSMC 180 nm RFCMOS process. Fig. 3 (a) shows the detailed simulation modeling of the antenna and (b) fabricated chip within the boundary of the chip antenna.

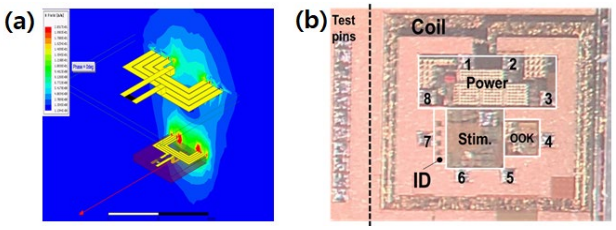

Fig. 3. (a) RF field simulation result and (b) photograph image of fabricated wireless electroceutical chip.

The power management circuit incorporates a 2-stage bridge rectifier with 5 pF charging capacitors, alongside a capless LDO regulator that modulates the 900-915 MHz carrier frequency. The rectifier produces a DC output of 1.17V from 3 dBm of input power. The capless regulator is activated once the rectifier provides sufficient power. This controller guarantees a constant supply voltage for the ICs for recording stimulation and spikes. The regulator is composed of a conventional PASS transistor, an error amplifier, a start-up circuit, and a reference voltage generator. It is designed to achieve a target gain of over 80 dB and a phase margin of 60°.

The proposed neural implants demand that each IC have an up/down transceiver since they have independent communication with external devices. Backscatter communication is widely used in biomedical implants, and we utilize backscattering modulation for uplink communication in the recording IC. Placed at the rectifier's input port, an NMOS transistor modulates the matching impedance of the antenna. The transistor size is determined based on its parasitic capacitance and resistance. Calculation of the modulation frequency depends on the signal rate. While still allowing for detectable signal variations, the limited backscattering turn-on period guarantees stable VDD free from major fluctuations.

For downlink communication in the stimulation IC, an envelope detection circuit with an additional passive low-pass filter (LPF) is employed. Working at a 915 MHz carrier frequency, the on-off keying (OOK) demodulation circuit sends the demodulated signal to a comparator. Additionally, an internal ring oscillator provides the clock signal to the comparator and digital logic, helping to reduce the bit error rate. The overall system schematic is shown in Fig. 4.

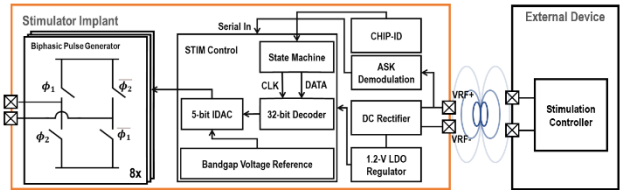

Fig. 4. Block diagram of addressable microstimulator with Chip-ID and on-chip coil antenna.

Table I shows the detailed performance of the system and comparison to existing works related to current stimulation for electroceutical applications.

TABLE I. Performance comparison between our system and existing works

	This work	StimDust (2020) [13]	Multisite VNS implants (2023) [14]	Neurograin (2024) [15]
Mode	Biphasic current	Current-controlled biphasic pulses	Biphasic voltage pulses	Biphasic current
Supply voltage	1.2 V	~1.8 V	~ 3.3 V	~1.0 V
Channel	8	1	2	1
Current	120 µA	~100 µA (constant current)	-	~ 120 µA
Pulse width	50 µs – 1 ms	50–500 µs	≥100 µs	100–200 µs
Frequency	5 – 1 kHz	1–2200 Hz	~50 Hz	1–2000 Hz
Power Consumption	9.7 µW / 2.1 mW	~4 µW idle	27 µW idle / ~1 mW	~<10 µW
Power & Data Transmission	RF / On-chip coil	Ultrasound-powered (piezo); & backscatter uplink	Inductive resonant link (13-14 MHz) / ASK data modulation	1 GHz RF inductive powering; ASK/PWM downlink / BPSK backscatter uplink
Area	1mm^2	~1.0 mm^2	0.75 × 1.6 mm	~0.25 mm^2
ID	Anti-fuse	-	PCB-defined passcode	On-chip ID
CMOS technology	180nm	65 nm CMOS	180 nm CMOS	65 nm CMOS

III. RESULTS AND DISCUSSIONS

Fig. 5 (a) shows DC rectifier and capless LDO regulator providing stable 1.17V to the system, providing constant system operation, and (b) shows OOK demodulation of the RF signal. The result indicates that a low-pass filter reduces the amplitude of PREDATA. Still, it is enough for demodulation since the comparator obtained 320 mV as reference voltage below the PREDATA. The minimum amplitude detected for demodulation was 350 mV, regenerating 1 MHz clock. An extra D-Flip-flop synchronized the DATA and CLK while the system clock, 1.07 MHz was split from a 12 MHz ring oscillator. 915MHz resonant chip coil receives data and power.

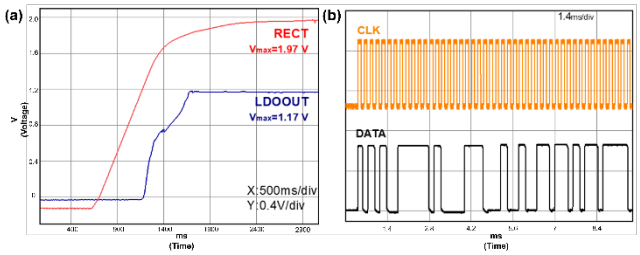

Fig. 5. (a) Power Management Integrated Circuit (PMIC) performance of the fabricated chip and (b) wireless data transmission using the inductive coupling method.

The chip was successfully turned on in a preclinical study involving rabbits, thus verifying the effective delivery of the stimulation waveforms to the nervous systems of the animals. Fig. 6 (a) shows the preclinical verification of the system, implanted in the rabbit. The chip was attached to the vagus nerve, and follow-up observations will be conducted to investigate physiological changes and response mechanisms. This method shows the practical viability of electroceutical technology in an animal model and is expected to offer important information for next therapeutic uses and clinical assessments. Fig. 6 (b) and (c) show the real-time waveforms recorded from the stimulation chip connected to the rabbit.

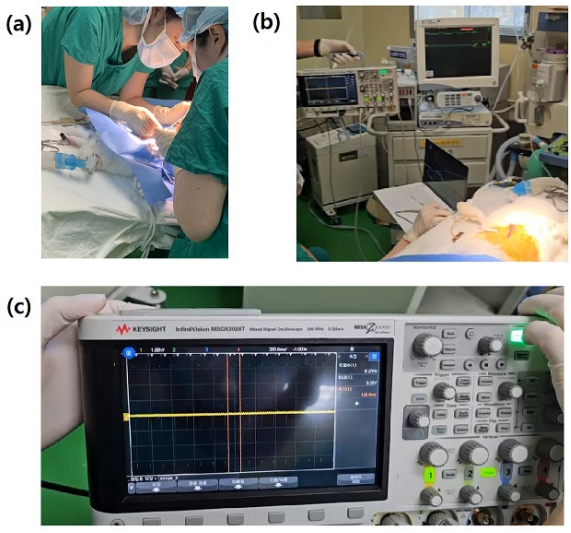

Fig. 6. (a) Preclinical implantation of the chip into a rabbit, (b) overall testing setup, and (c) Stimulation pulse of the implanted chip.

IV. CONCLUSIONS

The suggested system shows good design decisions for the integration of stimulation, communication, and power management features. Combining a two-stage bridge rectifier with a 5 pF charging capacitor and a capless LDO regulator guarantees a continuous and effective power supply to the system, so transforming the 900-915 MHz RF carrier into a useable 1.17 V DC output with 3 dBm input power. Both the stimulus and recording ICs run on this power, which guarantees steady operation without a large battery system. Combined with the PASS transistor, error amplifier, start-up circuit and reference voltage generator, the capless LDO regulator offers a stable supply voltage with a gain of more than 80 dB and a phase margin of 60°, so maximizing the performance of the stimulus IC and spike recording IC. For communication, the system utilizes backscatter modulation for uplink communication, with the NMOS transistor modulating the antenna's matching impedance based on parasitic capacitance and resistance. This guarantees constant VDD levels and effective signal transmission. The modulation frequency, linked to the spike rate, ensures that the backscattering turn-on period remains narrow enough to avoid destabilizing the system's power supply while still producing a detectable signal.

OOK demodulation at a 915 MHz carrier frequency combined with passive low-pass filter (LPF) implementation helps to detect envelopes for the downlink communication in the stimulation IC. The demodulated signal is then sent to a comparator, which receives a clock signal from the internal ring oscillator to reduce the bit error rate. Within the digital logic, the demodulated binary signal is utilized for clock synchronizing among counters and registers, producing the sequential switching signal required to regulate the programmable stimulation pulse.

The system offers a high level of flexibility with an on-chip 4-bit DAC for controlling the current amplitude, generating timing signals for pulse width and frequency, and setting the current direction through the biphasic pulse generator. These elements taken together provide a small neural implant architecture fit for effective, dependable, and power-efficient stimulation and communication in biomedical applications. Combining backscatter communication, power-efficient data transmission, and precise stimulation control demonstrates the feasibility of a system suitable for long-term, reliable neural implants without the need for frequent battery replacement.

The implant was attached to the rabbit vagus nerve, and the transmitted stimulation waveform was accurately replicated in vivo, with no noticeable loss of waveform amplitude or timing skew during the trial session—evidence of sufficient signal integrity under physiological loading—all of which are supported by acute pre-clinical testing. To assess treatment effectiveness, follow-up research will monitor autonomic indicators, such as body weight loss.

The device has been fully fabricated using a 180 nm RFCMOS process, with its inductive coil implemented in the top-metal layer. This configuration is compatible with common hermetic packaging strategies, such as metal/ceramic lids or thin-film Parylene C, although long-term experiments are still ongoing. To ensure multi-year

biocompatibility, future research will include mechanical robustness, ionic-leakage suppression, and the long-term reliability of encapsulation.

ACKNOWLEDGMENT

The chip fabrication and EDA tools were supported by the IC Design Education Center(IDEC), Korea. This research was supported by the Basic Science Research Program through the National Research Foundation of Korea(NRF) funded by the Ministry of Education(RS-2022-NR070876).

REFERENCES

[1] Y. Long, J. Li, F. Yang, J. Wang, and X. Wang, "Wearable and Implantable Electroceuticals for Therapeutic Electrostimulations," *Adv. Sci.*, vol. 8, no. 8, pp. 1–22, 2021, doi: 10.1002/advs.202004023.

[2] A. A. Mutah, J. Amitrano, M. A. Seeley, and D. Seshadri, "A Review of Wearable Electroceutical Devices for Chronic Wound Healing," 2025.

[3] C. Qin, Z. Yue, G. G. Wallace, and J. Chen, "Bipolar Electrochemical Stimulation Using Conducting Polymers for Wireless Electroceuticals and Future Directions," *ACS Appl. Bio Mater.*, vol. 5, no. 11, pp. 5041–5056, 2022, doi: 10.1021/acsabm.2c00679.

[4] S. M. Won, L. Cai, P. Gutruf, and J. A. Rogers, "Wireless and battery-free technologies for neuroengineering," *Nat. Biomed. Eng.*, vol. 7, no. 4, pp. 405–423, 2023, doi: 10.1038/s41551-021-00683-3.

[5] L. Lyu *et al.*, "A Fully-Integrated 64-Channel Wireless Neural Interfacing SoC Achieving 110 dB AFE PSRR and Supporting 54 Mb/s Symbol Rate, Meter-Range Wireless Data Transmission," *IEEE Trans. Circuits Syst. II Express Briefs*, vol. 67, no. 5, pp. 831–835, 2020, doi: 10.1109/TCSII.2020.2982208.

[6] N. Zeng *et al.*, "A Wireless, Mechanically Flexible, 25μm-Thick, 65,536-Channel Subdural Surface Recording and Stimulating Microelectrode Array with Integrated Antennas," *Dig. Tech. Pap. - Symp. VLSI Technol.*, vol. 2023-June, pp. 1–2, 2023, doi: 10.23919/VLSITechnologyandCir57934.2023.10185321.

[7] L. Zhao, W. Shi, Y. Gong, X. Liu, W. Li, and Y. Jia, "33.9 A Miniature Neural Interface Implant with a 95% Charging Efficiency Optical Stimulator and an 81.9dB SNDR ΔΣM-Based Recording Frontend," *Dig. Tech. Pap. - IEEE Int. Solid-State Circuits Conf.*, vol. 67, pp. 558–560, 2024, doi: 10.1109/ISSCC49657.2024.10454382.

[8] M. M. Ghanbari *et al.*, "A Sub-mm3 Ultrasonic Free-Floating Implant for Multi-Mote Neural Recording," *IEEE J. Solid-State Circuits*, vol. 54, no. 11, pp. 3017–3030, 2019, doi: 10.1109/JSSC.2019.2936303.

[9] A. A. Neural *et al.*, "Communication with Direct Analog to Time Conversion," pp. 209–212, 2022.

[10] Y. Shen *et al.*, "A Battery-Free Neural-Recording Chip Achieving 5.5 cm Fully-Implanted Depth by Galvanically-Switching Passive Body Channel Communication," *IEEE J. Solid-State Circuits*, vol. 59, no. 8, pp. 2591–2603, 2024, doi: 10.1109/JSSC.2024.3366176.

[11] C. Lee *et al.*, "A Miniaturized Wireless Neural Implant With Body-Coupled Power Delivery and Data Transmission," *IEEE J. Solid-State Circuits*, vol. 57, no. 11, pp. 3212–3227, 2022, doi: 10.1109/JSSC.2022.3202795.

[12] J. Lim *et al.*, "A 0.19×0.17mm2 Wireless Neural Recording IC for Motor Prediction with Near-Infrared-Based Power and Data Telemetry," *IEEE J. Solid-State Circuits*, vol. 57, no. 4, pp. 1061–1074, 2022, doi: 10.1109/JSSC.2022.3141688.

[13] D. K. Piech *et al.*, "A wireless millimetre-scale implantable neural stimulator with ultrasonically powered bidirectional communication," *Nat. Biomed. Eng.*, vol. 4, no. 2, pp. 207–222, 2020, doi: 10.1038/s41551-020-0518-9.

[14] I. Habibagahi, J. Jang, and A. Babakhani, "Miniaturized Wirelessly Powered and Controlled Implants for Multisite Stimulation," *IEEE Trans. Microw. Theory Tech.*, vol. 71, no. 5, pp. 1911–1922, 2023, doi: 10.1109/TMTT.2022.3233368.

[15] A. H. Lee, J. Lee, V. Leung, L. Larson, and A. Nurmikko, "Patterned electrical brain stimulation by a wireless network of implantable microdevices," *Nat. Commun.* , vol. 15, no. 1, 2024, doi: 10.1038/s41467-024-54542-1.

Joonyoung Lim received a B.S. degree in Nanoscience Engineering from Yonsei University, Seoul, Korea, in 2020 and is currently working toward an Integrated M.S. and Ph.D. degree at Seoul National University, Korea. His main interest is designing and applying functional analog front-end in the Brain-Machine Interface system.

Yoon-Kyu Song received the B.S. and M.S. degrees in Electrical Engineering from Seoul National University, Korea, in 1992 and 1994, respectively, and the Ph.D. degree from Brown University, Providence, RI, in 1999.

His research interests include applied neural engineering, such as brain-machine interfaces and electroceuticals.